






Boosting Neutrino Mass Ordering Sensitivity with Inelasticity for Atmospheric Neutrino Oscillation Measurement

Santiago Giner Olavarrieta ^{1,*} Miao Chen Jin (靳淼辰) ^{1,†}
 Carlos A. Argüelles ^{1,‡} Pablo Fernández ^{2,§} and Ivan Martinez-Soler ^{3,¶}

¹*Department of Physics & Laboratory for Particle Physics and Cosmology,
 Harvard University, Cambridge, MA 02138, USA*

²*Donostia International Physics Center DIPC, San Sebastián/Donostia, E-20018, Spain*

³*Department of Physics & Institute for Particle Physics Phenomenology,
 University of Durham, Durham, DH1 3LE, United Kingdom*

(Dated: February 22, 2024)

In this letter, we study the potential of boosting the atmospheric neutrino experiments sensitivity to the neutrino mass ordering (NMO) sensitivity by incorporating inelasticity measurements. We show how this observable improves the sensitivity to the NMO and the precision of other neutrino oscillation parameters relevant to atmospheric neutrinos, specifically in the IceCube-Upgrade and KM3NeT-ORCA detectors. Our results indicate that an oscillation analysis of atmospheric neutrinos including inelasticity information has the potential to enhance the ordering discrimination by several units of χ^2 in the assumed scenario of 5 and 3 years of running of IceCube-Upgrade and KM3NeT-ORCA detectors, respectively.

Introduction— Unmagnetized neutrino experiments cannot distinguish neutrinos from antineutrinos on an event-by-event basis when studying neutrino-nucleon interactions. Instead, experiments operating without a magnet need to rely on the particle content of the beam or the use of kinematic observables to statistically separate neutrinos from antineutrinos.

So far, analysis of atmospheric neutrinos aimed to determine neutrino oscillation parameters [1–4] has not exploited kinematic variables aimed at distinguishing between neutrinos and antineutrinos in large telescopes based on water/ice-Cherenkov.

This missing information undoubtedly hides the potential of atmospheric neutrinos in measuring the different oscillation effects that are distinct between neutrinos and antineutrinos, namely the mass ordering through the Mikheyev-Smirnov-Wolfenstein (MSW) [5, 6] Earth matter effects and the magnitude of the CP -violating phase in the lepton sector [7]. This is particularly important since, as recently demonstrated in Ref. [8], atmospheric neutrino experiments are expected to yield the most precise measurements of the neutrino oscillation parameters and are expected to determine the neutrino mass ordering by the end of the decade.

With this motivation, the Super-Kamiokande experiment has already implemented various techniques to distinguish neutrinos from antineutrinos [9]: detecting low-energy secondary particles like Michel electrons or neutrons, and computing kinematically relevant variables when possible, that is in the multi-ring samples. Producing a first neutrino oscillation analysis with neutrino-anti-neutrino event based on neutron tagging [10].

The former requires a low-background detector

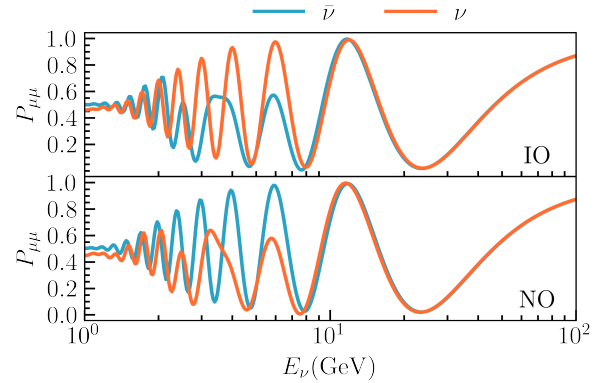


FIG. 1. Muon disappearance probabilities for both mass orderings, normal (NO) and inverted (IO), and both neutrinos and anti-neutrino, considering a trajectory crossing the entire Earth ($\cos \theta_\nu = -0.95$). As a best fit parameters, we used the results of latest global analysis [11]. A Gaussian filter with a width of $5\%\sqrt{E_\nu}$ has been included to remove the fast oscillations at lower energies.

* santiagoginer@college.harvard.edu

† miaochenjin@g.harvard.edu

‡ carguelles@fas.harvard.edu

§ pablo.fernandez@dipc.org

¶ ivan.j.martinez-soler@durham.ac.uk

with very high photo-sensor coverage, which is currently out of reach for the large, next-generation, multi-megatonne neutrino detectors. On the other hand, in this work, we demonstrate how the IceCube-Upgrade and KM3NeT-ORCA detectors could use the reconstructed inelasticity of the neutrino interaction to improve the sensitivity to neutrino mass ordering and the CP phase. The inelasticity y , also known as Bjorken- y , is the fraction of the neutrino energy transferred to a hadronic system with which the neutrino interacts. There are some efforts that has already been taken in the IceCube collaboration in reconstructing the inelasticity of low energy events [12]. Thus, in this letter, we extend the work in Ref. [8] by studying the impact in sensitivity of the IceCube-Upgrade and KM3NeT-ORCA neutrino telescopes that comes from incorporating an event's inelasticity in the oscillation analysis.

The results obtained in this work further complement the motivation of a combined oscillation analysis of atmospheric neutrinos to provide a precise picture of the mixing scenario independent from the current and early measurements of the next-generation accelerator experiments. As well as motivate the development of techniques that enable the reconstruction of the inelasticity in neutrino telescopes.

Atmospheric neutrinos and antineutrinos —

The study of neutrino oscillations has entered an era of high precision, where only a few aspects remain unknown. Among these unknowns are the octant of the θ_{23} , the mass ordering, and the CP -phase, δ_{CP} . Both the mass ordering and δ_{CP} predict different behaviors for neutrinos and anti-neutrinos as they propagate through Earth. Specifically, in the case of normal mass ordering (NO), where $m_3 > m_2, m_1$, a matter-induced resonance is predicted for neutrinos crossing the mantle and the core of the Earth at energies around 6 GeV. In the case of inverted ordering (IO), where $m_3 < m_1, m_2$, this resonance occurs in the anti-neutrino propagation, as illustrated in Figure 1. A similar situation arises in the case of δ_{CP} , where, in the presence of CP -violation, the oscillation evolution differs between neutrinos and antineutrinos. For a detailed description of the effects of CP -violation on atmospheric neutrino evolution, see [8].

The different oscillation patterns between neutrinos and anti-neutrinos suggest that the separation of both particle types in the event basis is the best way to explore the aforementioned parameters. In accelerator experiments, this is done by running the experiment in both the neutrino and anti-neutrino modes, while in the case of atmospheric neutrinos,

the flux contains both neutrino types. Therefore, we look for an alternative way to discriminate between neutrino- and anti-neutrino-type events.

Following a neutrino's charged-current (CC) interaction with a nucleon (N), the neutrino energy is split between the leptonic (l_α) and hadronic (h) currents, $\nu_\alpha + N \rightarrow l_\alpha + h$. The $V - A$ structure of the weak tensor in the case of the neutrino interaction results into a different cross-section for neutrinos and anti-neutrinos [13], when neutrinos interact primarily with valence quarks, which is the case at the relevant energies. Considering just the case where the neutrinos interact via Deep-Inelastic Scattering (DIS), the relevant component above 3 GeV, and following the notation in [14], the neutrino cross-section can be written in terms of the inelasticity ($y = 1 - E_l/E_\nu$), where E_l is the energy of the outgoing lepton, and the Bjorken scaling variable (x) as

$$\frac{d\sigma_\nu^{CC}}{dydx} = \frac{G_F^2 xs}{2\pi} (Q(x) + \bar{Q}(x) \times (1 - y)^2), \quad (1)$$

$$\frac{d\sigma_{\bar{\nu}}^{CC}}{dydx} = \frac{G_F^2 xs}{2\pi} (\bar{Q}(x) + Q(x) \times (1 - y)^2), \quad (2)$$

where G_F is the Fermi constant and s is the square of the center-of-mass energy. The symbols $Q(x)$ and $\bar{Q}(x)$ corresponds to the sum of all the parton distribution functions (PDFs) for quarks and anti-quarks that contribute to the nucleons. To explore the dependence of the neutrino cross-section on the inelasticity, we have integrated the double differential cross-section over x within the kinematic allowed region, and using the PDF4LHC21 set [15] PDFs set. We find an almost uniform energy distribution of the outgoing lepton in the case of the neutrino interaction, as shown in Figure 2. In the case of

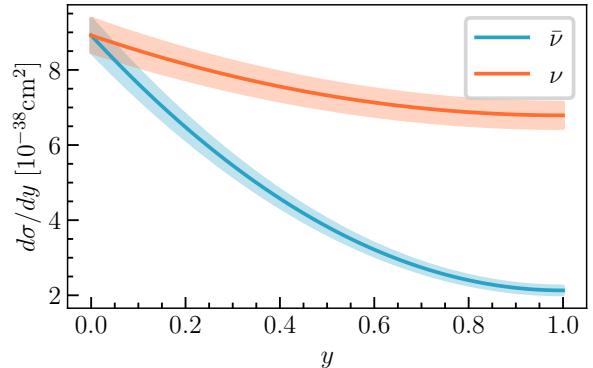


FIG. 2. Differential neutrino charge current cross-section for the DIS regime. The shaded region corresponds to the 1σ uncertainty region included for DIS in this analysis.

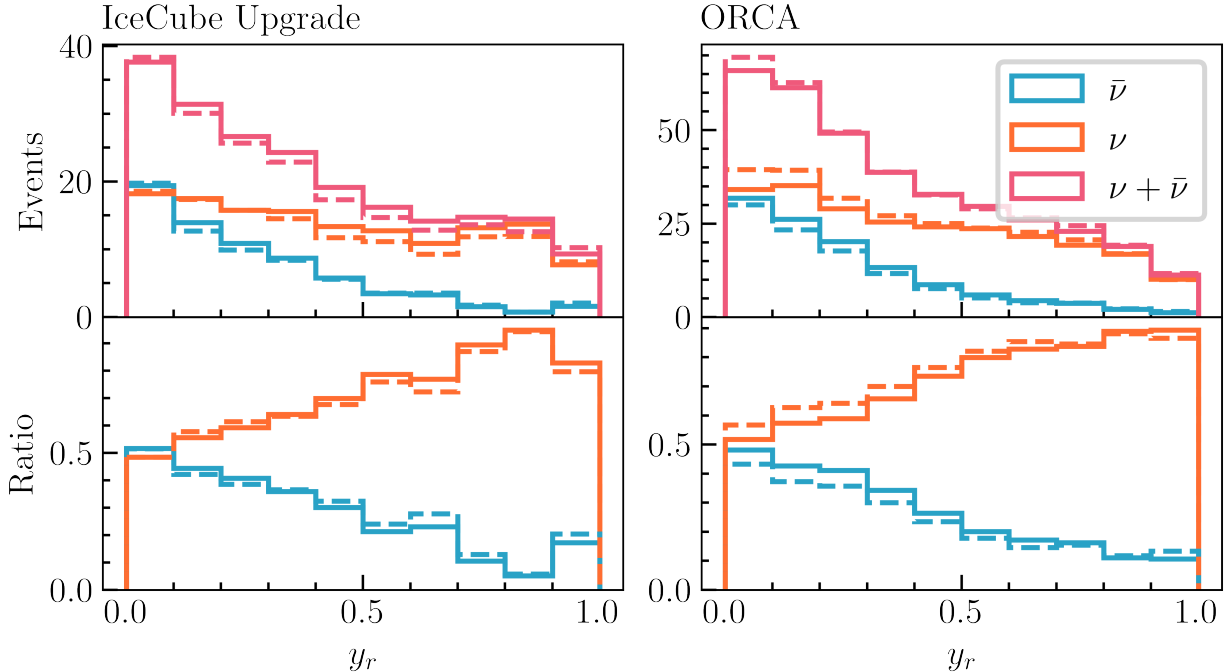


FIG. 3. Histogram of events in IceCube Upgrade and ORCA as a function of y_r for a bin in $E_r \in [5.0, 6.3]$ GeV and $\cos \theta_r \in [-0.8, -0.6]$. The solid line corresponds to Normal Ordering and the dashed line to Inverted Ordering. In the lower panel, we display the ratio between the neutrinos (orange) and anti-neutrinos (blue) and the total number of events for both normal and inverted ordering.

the anti-neutrino interaction, most of the energy of the incoming neutrino is carried out by the outgoing lepton. Therefore, it is possible to get a large neutrino-anti-neutrino separation for large values of y .

Although we have restricted the discussion in this section to the DIS interaction, all the results that are presented in this analysis are based on simulations that includes all the interaction channels, as described in [8].

Experiments and Methods— The IceCube Neutrino Observatory [16] is an ice-Cherenkov neutrino detector located on average 2 km below the surface at the geographic South Pole. It consists of 5160 light sensors known as digital optical modules (DOMs) that allow it to detect neutrino interactions above ~ 10 GeV. Depending on the type of particle propagating through the ice, an event will correspond to one of two possible morphologies, namely, *tracks*, coming from the propagation of muons, and *cascades*, coming from the propagation of electrons, taus, and/or hadronic or electromagnetic cascades. In the near future, a detector upgrade [17, 18] that will consist in the deployment of additional strings allowing to lower the energy threshold to a few GeV.

We further consider the ORCA detector, which is part of the KM3NeT water-Cherenkov neutrino telescope currently under construction in the Mediterranean Sea [19]. As in the case of IceCube, ORCA also identifies tracks and cascades as possible event morphologies, but have also developed a third sample, namely, the *intermediate*, for events that cannot be clearly identified as part of the former two. For the purposes of our analysis, we use the open-access Monte Carlo simulation of ORCA developed in [8], which is built as an extension of the open-access IceCube-Upgrade Monte Carlo release.

In both experiments, we compute the inelasticity for charged-current ν_μ events which produce an outgoing muon, reconstructed as a track, and a hadronic shower, identified as a cascade. In terms of reconstructed quantities,

$$y_r = \frac{E_r^{\text{casc}}}{E_r^{\text{casc}} + E_r^{\text{track}}}. \quad (3)$$

Current oscillation analysis carried away by IceCube and ORCA use a two-dimensional histogram of the events in terms of the reconstructed energy and the direction for each morphological category. To incorporate the inelasticity in the analysis, we

modified the Monte Carlo simulations for IceCube-Upgrade [20] and ORCA by adding a variable corresponding to the reconstructed inelasticity, y_r . For every MC event reconstructed as a track, we generate a set of N additional events, where the inelasticity is reconstructed based on the reconstructed energy for the track and the cascade. For the main results of this work, we have assumed a Gaussian distribution with uncertainty of $\sigma_T = 20\%$ for tracks and $\sigma_C = 30\%$ for cascades. For the main results of this work, we have assumed a Gaussian distribution with uncertainty of $\sigma_T = 20\%$ for tracks and $\sigma_C = 30\%$ for cascades [4]. For the purposes of this letter, we used the case of $N = 20$ for the IceCube simulation and $N = 10$ for ORCA ¹.

In addition to the binning scheme described in [8], a third dimension is implemented for track events of both experiments, including 10 bins for the reconstructed inelasticity. An example of the event distribution we predict is shown in Figure 3, where we have chosen one bin in zenith $\cos \theta_r \in [-0.8, -0.6]$ and energy $E_r \in [5.0, 6.3]$ GeV. As anticipated from the previous discussion, for large values of y , the event distribution is primarily dominated by the neutrino sample. In the case of anti-neutrinos, the event distribution is concentrated in the bins with small y_r . The event distribution is depicted for both mass orderings, normal (solid), and inverted (dash). For neutrinos, the mass ordering induce a event deviation which is almost uniform in y_r . For the case of anti-neutrino, this deviation concentrates at lower y_r .

Analysis and Results — We have investigated how the sensitivity to oscillation parameters improves with the inclusion of inelasticity in the analysis. Through a combined analysis using currently publicly available IceCube-Upgrade and ORCA simulations, we have explored the sensitivity to the less constrained oscillation parameters— $\sin \theta_{23}$, mass ordering, and the CP-phase. In this work, we have kept the solar parameters (Δm_{21}^2 and $\sin^2 \theta_{12}$) and the reactor angle ($\sin^2 \theta_{13}$) fixed at their best-fit values [11]. Regarding systematic uncertainties, we have taken into account uncertainties associated with the atmospheric neutrino flux, neutrino cross-section, and detector response. These uncertainties have been included in the analysis in a manner similar to that presented in [8].

¹ We explored the sensitivity considering different values for N between $N = 10$ and $N = 100$, finding no significant deviation of the results.

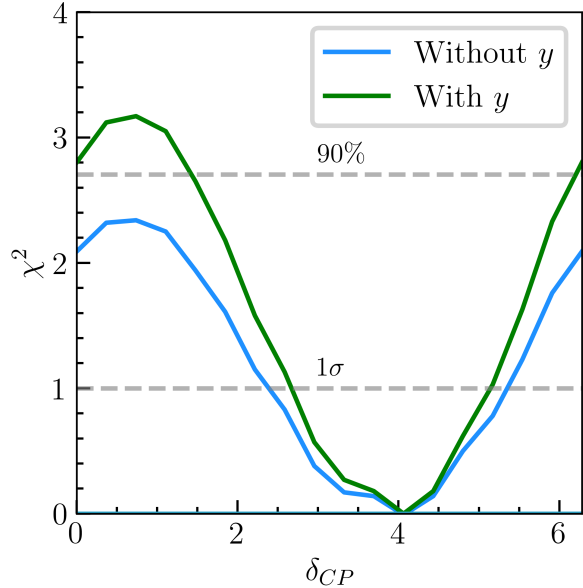


FIG. 4. Comparison of the sensitivity from the combined analysis of Icecube-Upgrade (5 years) and ORCA (3 years) to δ_{CP} (solid lines) incorporating the y_r binning (green) and the usual analysis (blue), assuming true normal ordering.

The main results of the combined analysis are illustrated in Figures 4 and 5. The sensitivities depicted correspond to the combination of IceCube-Upgrade and ORCA, with exposures of 5 and 3 years, respectively. In both figures, we assume normal ordering as the benchmark scenario. Regarding $|\Delta m_{31}^2|$, we observed an improvement of more than 30%, achieving a precision below the percent level (0.7%), as depicted in Figure 5 (solid lines). However, for $\sin^2 \theta_{23}$, which is influenced by the neutrino angular resolution, no improvement is observed. For both parameters, profiling has been performed over δ_{CP} and the parameters not shown.

The sensitivity to the ordering is depicted in Figure 5 by the dashed lines. We fit the event distribution assuming inverted ordering to the normal ordering scenario. The combination of IceCube Upgrade and ORCA will enable us to predict a 7σ exclusion of the inverted ordering without including the inelasticity, as shown in [8]. With the inclusion of inelasticity in the analysis, the sensitivity increases to $\sim 8.4\sigma$. When considering each experiment separately, IceCube Upgrade can reach $\sim 5\sigma$ in 3.5 years, while ORCA can do it in 2.5 years.

Finally, in the context of the CP-violating phase, although it does not have a significant impact on

the muon disappearance channel, the inclusion of inelasticity in the analysis increases the resolution of δ_{CP} by $\sim 15\%$.

Furthermore, to assess the resilience of our results, we investigated how the new sensitivity changes under limitations related to energy reconstruction and the possible misclassification of events with large inelasticity. These tests confirmed the robustness of our method to these potential errors; refer to the Appendix for detailed information.

Conclusion — In this letter, we introduced a novel approach to the oscillation analysis of the atmospheric neutrino data suitable for the upcoming IceCube-Upgrade and ORCA experiments. We motivate and demonstrate that introducing the information of the reconstructed inelasticity of track events has the potential to discern neutrinos and anti-neutrinos in the few GeV region, thus impacting the sensitivity of the relevant oscillation parameters, namely the neutrino mass ordering, the squared mass difference and the CP-phase. This results motivate

the development of reconstruction techniques that can infer the inelasticity for sub-100 GeV energies.

This work builds up the results from [8] showing the relevant role of atmospheric neutrinos in unequivocal measuring the neutrino mass ordering before the end of the decade and constraining the allowed values for the remaining oscillation parameters independently from the long-baseline programs.

Acknowledgments — SG acknowledges support from the Harvard College Research Program in the fall of 2023. CAA are supported by the Faculty of Arts and Sciences of Harvard University, the National Science Foundation, IAIFI, and the David & Lucile Packard Foundation. CAA and IMS were supported by the Alfred P. Sloan Foundation for part of this work. MJ is supported by the National Science Foundation and the Faculty of Arts and Sciences of Harvard University. IMS is supported by STFC grant ST/T001011/1.

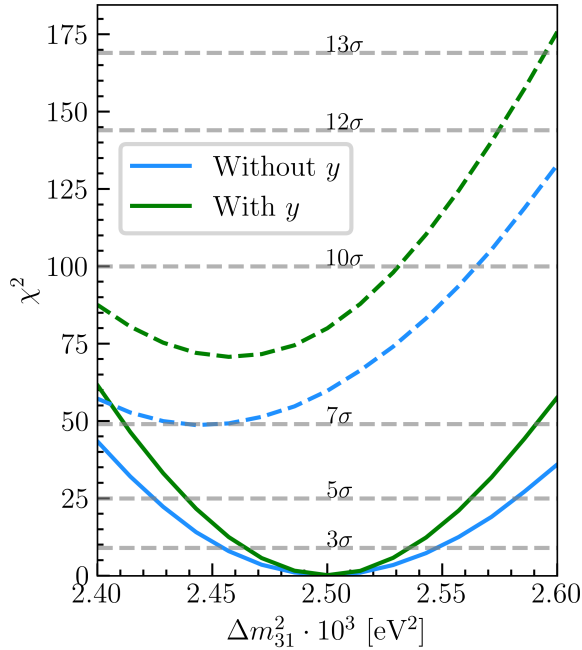


FIG. 5. Comparison of the sensitivity from the combined analysis of Icecube-Upgrade (5 years) and ORCA (3 years) to Δm_{31}^2 (solid lines) incorporating the y_r binning (green) and the usual analysis (blue), assuming true normal ordering. Dashed lines are the inverted ordering fit, showing the NMO sensitivity in units of χ^2 as a function of Δm_{31}^2 . In this analysis, we have profiled over $\sin \theta_{23}$ and δ_{CP} , maintaining their best fit equal to the latest result from the global analyses.

-
- [1] K. Abe *et al.* (Super-Kamiokande), Atmospheric neutrino oscillation analysis with external constraints in Super-Kamiokande I-IV, *Phys. Rev. D* **97**, 072001 (2018), [arXiv:1710.09126 \[hep-ex\]](#).
 - [2] A. Albert *et al.* (ANTARES), Measuring the atmospheric neutrino oscillation parameters and constraining the 3+1 neutrino model with ten years of ANTARES data, *JHEP* **06**, 113, [arXiv:1812.08650 \[hep-ex\]](#).
 - [3] V. Pestel, L. Nauta, and Z. Aly (KM3NeT), First neutrino oscillation measurement with KM3NeT/ORCA, *PoS NuFact2021*, 064 (2022).
 - [4] R. Abbasi *et al.* ((IceCube Collaboration)*, IceCube), Measurement of atmospheric neutrino mixing with improved IceCube DeepCore calibration and data processing, *Phys. Rev. D* **108**, 012014 (2023), [arXiv:2304.12236 \[hep-ex\]](#).
 - [5] L. Wolfenstein, Neutrino Oscillations in Matter, *Phys. Rev. D* **17**, 2369 (1978).
 - [6] S. P. Mikheyev and A. Y. Smirnov, Resonance Amplification of Oscillations in Matter and Spectroscopy of Solar Neutrinos, *Sov. J. Nucl. Phys.* **42**, 913 (1985).
 - [7] S. Razzaque and A. Y. Smirnov, Super-PINGU for measurement of the leptonic CP-phase with atmospheric neutrinos, *JHEP* **05**, 139, [arXiv:1406.1407 \[hep-ph\]](#).
 - [8] C. A. Argüelles, P. Fernández, I. Martínez-Soler, and M. Jin, Measuring Oscillations with a Million Atmospheric Neutrinos, *Phys. Rev. X* **13**, 041055 (2023), [arXiv:2211.02666 \[hep-ph\]](#).
 - [9] K. Abe *et al.* (Super-Kamiokande), Neutron tagging following atmospheric neutrino events in a water Cherenkov detector, *JINST* **17** (10), P10029, [arXiv:2209.08609 \[hep-ex\]](#).
 - [10] T. Wester *et al.* (Super-Kamiokande), Atmospheric neutrino oscillation analysis with neutron tagging and an expanded fiducial volume in Super-Kamiokande I-V, (2023), [arXiv:2311.05105 \[hep-ex\]](#).
 - [11] I. Esteban, M. C. Gonzalez-Garcia, M. Maltoni, T. Schwetz, and A. Zhou, The fate of hints: updated global analysis of three-flavor neutrino oscillations, *JHEP* **09**, 178, [arXiv:2007.14792 \[hep-ph\]](#).
 - [12] J. H. Peterson, M. P. Rodriguez, and K. Hanson (IceCube), 2D Convolutional Neural Network for Event Reconstruction in IceCube DeepCore, *PoS ICRC2023*, 1129 (2023), [arXiv:2307.16373 \[astro-ph.HE\]](#).
 - [13] M. Ribordy and A. Y. Smirnov, Improving the neutrino mass hierarchy identification with inelasticity measurement in PINGU and ORCA, *Phys. Rev. D* **87**, 113007 (2013), [arXiv:1303.0758 \[hep-ph\]](#).
 - [14] F. Halzen and A. D. Martin, *QUARKS AND LEPTONS: AN INTRODUCTORY COURSE IN MODERN PARTICLE PHYSICS* (1984).
 - [15] R. D. Ball *et al.* (PDF4LHC Working Group), The PDF4LHC21 Combination of Global PDF Fits for the LHC Run III, *J. Phys. G* **49**, 080501 (2022), [arXiv:2203.05506 \[hep-ph\]](#).
 - [16] A. Achterberg *et al.* (IceCube), First year performance of the IceCube neutrino telescope, *Astroparticle Physics* **26**, 155–173 (2006).
 - [17] A. Ishihara (IceCube), The IceCube Upgrade - Design and Science Goals, *PoS ICRC2019*, 1031 (2021), [arXiv:1908.09441 \[astro-ph.HE\]](#).
 - [18] T. Stuttard (IceCube), Neutrino oscillations and PMNS unitarity with IceCube/DeepCore and the IceCube Upgrade, *PoS NuFact2019*, 099 (2020).
 - [19] S. Adrián-Martínez *et al.* (KM3Net), Letter of intent for km3net 2.0, *Journal of Physics G: Nuclear and Particle Physics* **43**, 084001 (2016), 1601.07459.
 - [20] IceCube Collaboration (2020), *IceCube: Upgrade neutrino monte carlo simulation* (2020).
 - [21] P. Fernandez, I. Martínez-Soler, C. A. Argüelles, and J. Miao Chen, *Atmospheric Neutrino Monte Carlo Simulations* (2023).

Appendix A: Uncertainty Associated to the Inelasticity

In order to test the robustness of our results to different ways of modifying an experiment's Monte Carlo simulation when including the reconstructed inelasticity, y_r , we explored the NMO sensitivity obtained when y_r is drawn directly from a Gaussian distribution, instead of determined via the method described above relying on two separate Gaussian distributions for the reconstructed cascade and track energies. We describe this method in the current appendix, followed by its resulting sensitivity in Appendix B. As above, for every ν_μ CC interaction event having a true inelasticity of y , we create N additional events with an additional variable, y_r . Instead of computing y_r from reconstructed energies, we assume that

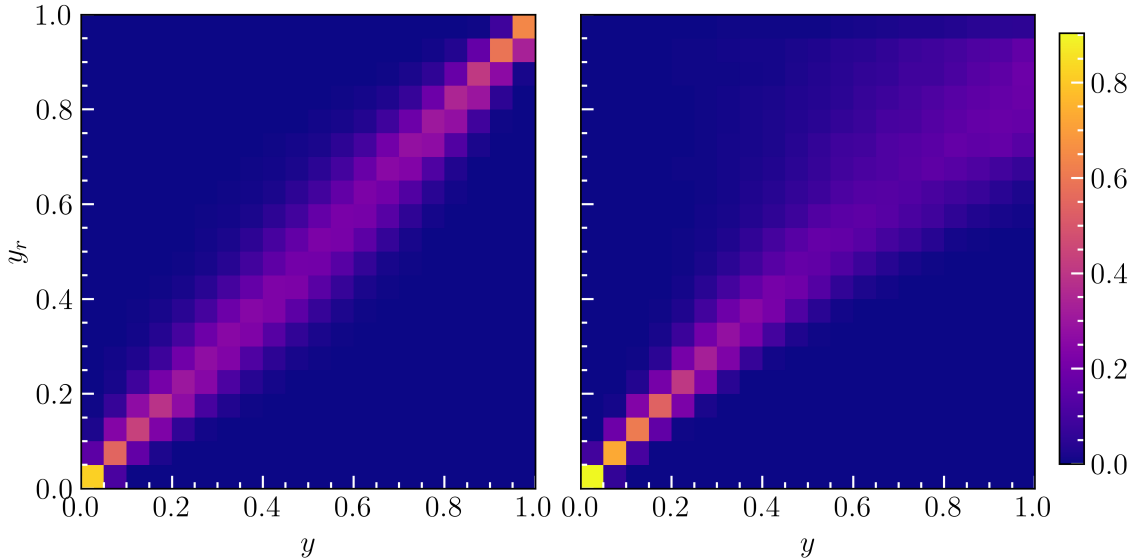
$$y_r \sim \mathcal{N}(y, \sigma_y), \quad (\text{A1})$$

where the standard deviation, σ_y , is given by

$$\sigma_y = y \sqrt{(1-y)^2 \sigma_L^2 + y^2 \sigma_H^2}. \quad (\text{A2})$$

Here σ_L and σ_H represent the magnitude of the error in the reconstruction of y for small and large values of y , respectively. To see why, notice that the factor multiplying y in the above approaches σ_L as $y \rightarrow 0$ and σ_H as $y \rightarrow 1$. We experimented with different values of these parameters and decided to use $(\sigma_L, \sigma_H) = (0.2, 0.3)$, for this would reproduce the errors used in the main analysis in the limits of low and high inelasticity, respectively. During the modification of an experiment's MC simulation, in the case that a draw from this distribution is outside the physical range $[0, 1]$, we simply continue taking draws from this distribution until we obtain a y_r value in this physical range.

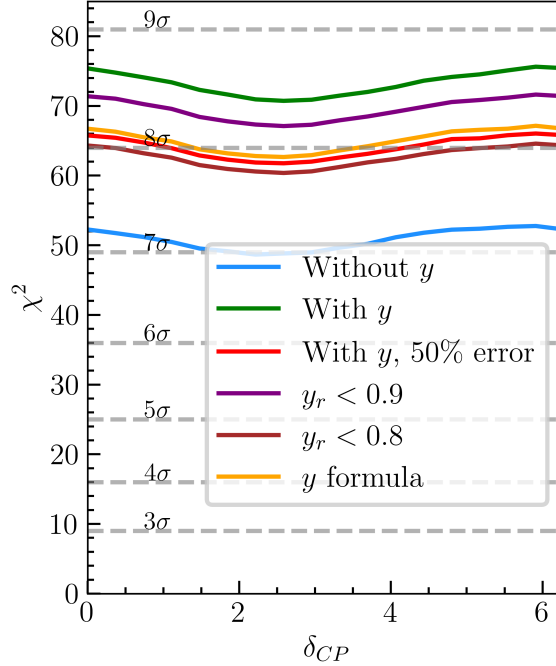
The distribution of y_r obtained using this method is plotted in [SUPPL. FIG. 1](#).



SUPPL. FIG. 1. Distribution of the reconstructed inelasticity, y_r , and the corresponding true value, y , in IceCube-Upgrade. The left plot corresponds to the modification of the MC explained in the main paper, where we draw samples from a Gaussian distribution for each of the reconstructed track and cascade energy, and calculate y_r from them. The right plot corresponds to the case where y_r is drawn directly from a Gaussian distribution, $y_r \sim \mathcal{N}(y, \sigma_y)$.

Appendix B: Impact of Inelasticity in the Oscillation Analysis

When assessing whether or not incorporating the inelasticity in the event analysis is worthwhile, two natural questions to ask are: (1) how robust is this method with respect to errors in the energy reconstruction of the track and cascade, and (2) is the resulting improvement in sensitivity coming only from bins with high y value, which could be misidentified as cascades by the reconstruction? Here we show how this proposed method is indeed robust to poor energy reconstruction and to misidentifications of events with large y as purely cascades. In SUPPL. FIG. 2, we show the impact that a poor reconstruction of the separate energies of the track and cascade would have on the resulting sensitivity to the mass ordering. We can see how, even making the very conservative assumption of a 50% error in the reconstruction of both the track's and the cascade's energy, there is still substantial improvement in the NMO sensitivity compared to the analysis that does not incorporate y at all. Therefore, our method is robust to errors in energy reconstruction.



SUPPL. FIG. 2. Combined NMO sensitivity of IceCube-Upgrade (5 yrs) and ORCA (3 yrs). The green line shows the sensitivity obtained by including the y and the blue is the usual analysis. The red line shows the case of poor energy reconstruction when inferring y_r , assuming a 50% error for both the track and cascade reconstructed energies. The purple and maroon lines show what happens when we only include the bins where $y_r < 0.9$ and $y_r < 0.8$, respectively, corresponding to the case where the high-inelasticity events are misclassified. Lastly, the orange line shows the sensitivity obtained when y_r is drawn directly from a Gaussian centered at each true y , as explained in Appendix A.

Furthermore, SUPPL. FIG. 2 shows what happens to the NMO sensitivity when we consider events with $y_r < 0.9$ and $y_r < 0.8$, that is, when we exclude high- y_r bins. This captures what would happen if all such events were incorrectly classified during the reconstruction. As in the case of poor energy reconstruction, the sensitivity decreases when we ignore this bin, but the overall value is still higher compared to the analysis that does not incorporate y . Thus, the improvement is robust to cases where the event morphology is classified incorrectly.